The differential cross section for dp-elastic scattering at 500-900 MeV/n and large transverse momenta

Arkady Terekhin[1,*], *Vladimir* Ladygin[1], *Yury* Gurchin[1], *Alexander* Isupov[1], *Marian* Janek[2], *Anatoliy* Khrenov[1], *Alexei* Kurilkin[1], *Pavel* Kurilkin[1], *Nadezhda* Ladygina[1], *Semeon* Piyadin[1], and *Sergey* Reznikov[1]

[1]Joint Institute for Nuclear Researches, Dubna 141980, Russia
[2]Physics Department, University of Žilina, Žilina 010 26, Slovak Republic

Abstract. The results of the differential cross section of elastic dp-scattering measurements at 500, 750 and 900 MeV/n, performed at the Internal Target Station at the JINR Nuclotron are presented. The angular dependence is compared with the world experimental data at close energies as well as with the theoretical calculations performed within the framework of the relativistic multiple scattering theory. The differential cross section at fixed scattering angles covered a total c.m. energy range $\sqrt{s}$ = 3.1 - 3.42 GeV were obtained. The results are compared with the behavior of the world data.

1 Introduction

The dp-elastic scattering process is the simplest example of the hadron nucleus collision. The study of the interactions mechanisms with involving a deuteron is aimed at obtaining the information on the role of relativistic effects, the contributions of Δ-isobars and quark degrees of freedom in nuclei. By now there are accumulated extensive experimental data and different theoretical models are developed. The experimental data cover the energy range from tens to thousands MeV/n [1]-[10]. Several approaches are exist to describe dp-scattering at the different energies. The approaches based on the solution of the three-particle Schroedinger equation [11–13] and on the Faddeev calculations [14, 15] are described of the three-nucleon scattering with high accuracy at the energies below 200 MeV/n [16, 17]. The different two- and three- nucleons forces are used in the theoretical calculations. The Glauber scattering theory which takes both single and double interactions is a classic approach at the energies higher than 400 MeV/n. [18, 19]. Now the approach based on the multiple-scattering theory which uses off-mass-shell extrapolations of the nucleon-nucleon amplitudes is developed [20, 21]. These calculations were applied to describe the dp-elastic scattering differential cross section at the energies up to 1000 MeV/n [21–24].

In recent years the experiments to study dp-elastic scattering were performed at the Internal Target Station (ITS) [25] at the JINR Nuclotron in the framework of DSS (Deuteron Spin Structure) project. The data for the differential cross section at 650, 700 [26] and 1000 MeV/n [27] were obtained. In this paper the angular dependences of the differential cross section for dp-elastic scattering at 500, 750 and 900 MeV/n, obtained at Internal Target Station (ITS) at the Nuclotron are presented.

*e-mail: aterekhin@jinr.ru

2 Experiment

The setup at the Internal Target Station at the Nuclotron allows one to obtain the different observables at the angular range 60-140° in the c.m.s. The measurements were performed using the unpolarized deuteron beam, the polyethylene (CH_2) and the carbon (^{12}C) targets. Two pairs of scintillation detectors placed symmetrically with respect to the beam direction were used to register the elastically-scattered deuterons and protons (*DP*-detectors). Also two monitor scintillation counters to detect products of *pp*-quasielastic scattering (*PP*-detectors). The dimensions of the scintillators in the P, D, and PP counters were 20×60×20, 10×40×24, and 50×50×10 mm, respectively. The distances from the proton, deuteron, and monitoring counters to the beam–target interaction point were 58, 56, and 56 cm, respectively. The layout of the counters with respect to the beam direction is shown in Fig. 1.

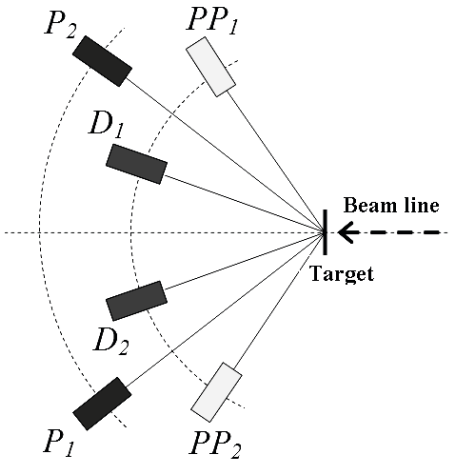

Figure 1. Layout of the counters with respect to the beam direction. $D_{1,2}$, $P_{1,2}$- deuteron and proton detectors, $PP_{1,2}$- detectors to register the pp-quasi-elastic scattering

The taking and recording the data from detectors were provide by the VME-system [28] which consist of two TQDC-16 16-channel modules, the TTCM-V2.0 triggering module, and the FVME-V1.0 controller. The data were collected at the energies 500, 650, 700, 750 and 900 MeV/n.

3 Differential cross section calculation

Energy losses in the scintillator and the particles time-of-flight are recorded as the amplitude and time signals. The dp-elastic scattering events were obtained by analysis of the amplitude spectra. The correlation of the deuteron and proton energy losses is shown in Fig. 2. The time difference ΔT_{d-p} between the arrival of signals from the D and P detectors is shown in Fig. 3.

The differential cross section was calculated as:

$$\left(\frac{d\sigma}{d\Omega}\right)_{c.m.} = \frac{N_{dp}}{d\Omega^D_{lab}} \frac{k_{pp}}{N_{CH_2}} J_D C_{norm}. \quad (1)$$

Here N_{dp} – the number of dp-elastic scattering events, $d\Omega^D_{lab}$ – the effective solid angle of the deuteron detector in the laboratory frame under the conditions of its kinematical coincidence

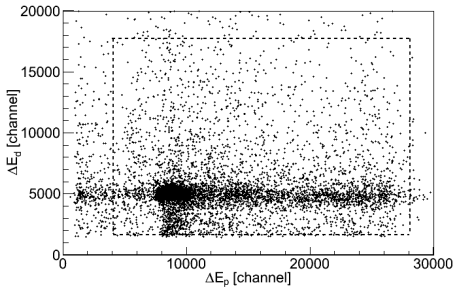

Figure 2. Correlation of the deuteron and proton energy losses at 500 MeV/n for $\theta_{c.m.} = 75°$. The dashed line represents the graphical criterion for separation of dp-elastic scattering events

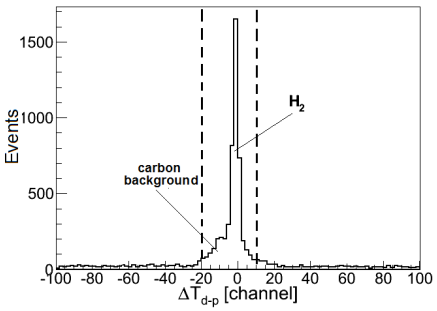

Figure 3. The time difference of the signals appearance from the deuteron and proton counters at scattering for $\theta_{c.m.} = 75°$ at 500 MeV/n

with the proton counter, N_{CH_2} – the number of reconstructed events for PP-counters under the condition of their coincidence with each other in the case of scattering on the polyethylene target, k_{pp} – the correction for the intensity of the carbon background in the N_{CH_2}, J_D – the transformation Jacobian for the transition from the laboratory to the c.m. frames and C_{norm} – the normalization coefficient.

The effective solid angle and the transformation Jacobian were calculated using of the Pluto event generator [29]. The N_{dp}, N_{CH_2}, k_{pp} were obtained from the experimental data. The number of the dp - elastic scattering events was calculated by using the CH_2-C subtraction procedure. The carbon amplitude distribution was normalized to the polyethylene spectrum in the domain where dp-elastic scattering does not contribute. After this, the normalized C - and CH_2 - spectra were subtracted.

The $CH_2 - C$ subtraction is not performed for the PP-detector data at each $\theta_{c.m.}$. The estimation of the intensity of the carbon background in scattering on polyethylene was performed for the data sum for all values of the angle $\theta_{c.m.}$. The coefficient k_{pp} was calculated as the ratio of the total number of pp-quasielastic events obtained on the CH_2 target without carbon background subtraction to the number of events after subtraction.

The normalization coefficients C_{norm} at 500 and 900 MeV/n were calculated by using the data at 700 MeV/n. The measurements at this energy were performed for the scattering angle $\theta_{c.m.} = 75.8°$. The obtained result for the differential cross section was normalized to the data [26] for the same angle. In order to calculate the normalization coefficient at the energy of 500(900) MeV/n, the correction R to the coefficient C^{700}_{norm} was introduced from the ratio of the differential cross sections for pp-elastic scattering at the energies 700 and 500(900) MeV/n in the region around the solid angle of the PP-detector. The normalization coefficient at the energy of 500(900) MeV/n was calculated as $C^{500(900)}_{norm} = C^{700}_{norm}/R$. Analogously the differential cross section at 750 MeV/n was calculated. The data at 650 MeV/n were used for the normalization coefficient C^{750}_{norm} calculation.

The angular dependences of the differential cross section at the energy of 500, 750 and 900 MeV/n compared with the world data at close energies and with the theoretical predictions are shown in Figs. 4, 5 and 6, respectively. The Nuclotron data are shown by closed squares, the data at 425 MeV/n [4] - by crosses, the data at 470 MeV/n [3] - by open squares,

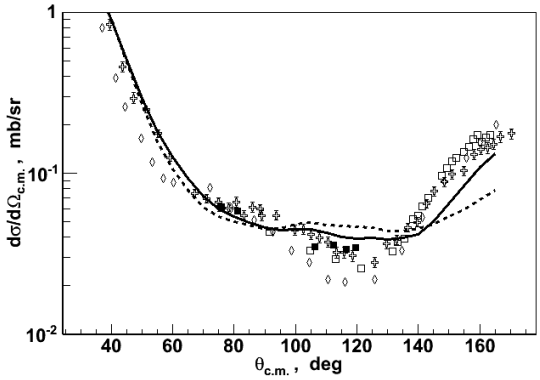

Figure 4. Differential cross section for dp-elastic scattering at 500 MeV/n. Solid squares – the Nuclotron data, crosses – the data at 425 MeV/n [4], diamonds – the data at 580 MeV/n [5], open squares – the data at 470 MeV/n [3], dashed and solid lines – the calculations without and with Δ-isobars, respectively, performed within the relativistic multiple-scattering model [24]

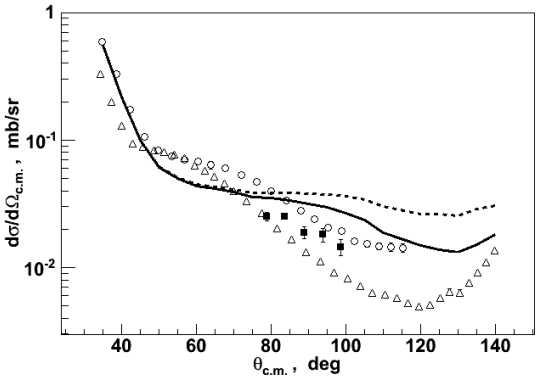

Figure 5. Differential cross section for dp-elastic scattering at 750 MeV/n. Solid squares – the Nuclotron data, circles and triangles – the data at 641 and 800 MeV/n [6], dashed and solid lines – the same as in Fig. 4

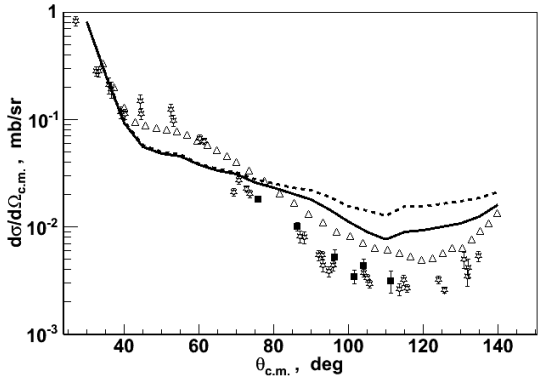

Figure 6. Differential cross section for dp-elastic scattering at 900 MeV/n. Solid squares – the Nuclotron data, triangles – data at 800 MeV/n [6], stars – the data at 1000 MeV/n [9], dashed and solid lines – the same as in Fig. 4

the data at 580 MeV/n [5] - by diamonds, the data at 641 MeV/n and 800 MeV/n [6] - by circles and triangles, respectively, the data at 1000 MeV/n [9] - by stars.

4 Differential cross section calculation at fixed angle scattering

At high energies and large transverse momenta the constituent counting rules (CCR) [30] predict the $1/s^{n-2}$ dependence of the differential cross section for the binary reaction, where n is the total number of the fundamental constituents involved in the reaction. For dp-elastic

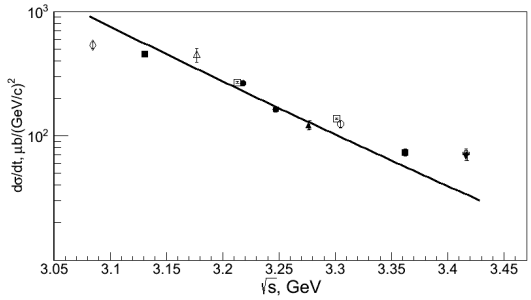

Figure 7. Differential cross section of dp-elastic scattering at fixed scattering angle of $\theta_{c.m.} \sim 75°$. Full symbols – the Nuclotron data, open symbols – the world data. Line – the result of the world data fitting by the function $\sim s^{-16}$

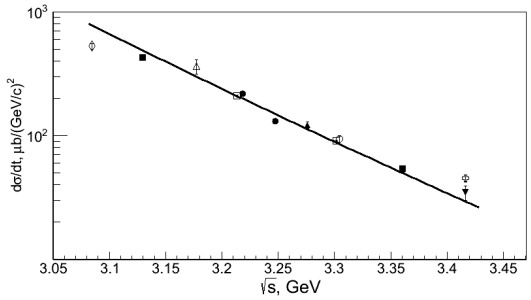

Figure 8. Differential cross section of dp-elastic scattering at fixed scattering angle of $\theta_{c.m.} \sim 82°$. Designations are the same as in Fig. 7

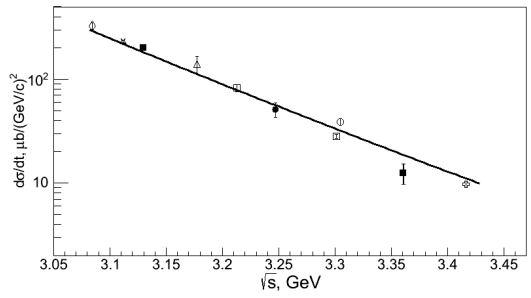

Figure 9. Differential cross section of dp-elastic scattering at fixed scattering angle of $\theta_{c.m.} \sim 111°$. Designations are the same as in Fig. 7

scattering $n = 18$. The differential cross section at three scattering angles of the c.m.s. covered the laboratory kinetic energy range 0.44 - 1 GeV corresponding to the total c.m. energies $\sqrt{s} = 3.1$ - 3.42 GeV are shown in Figs. 7, 8 and 9. The world data [3–6, 8, 9] are shown by the open symbols. The lines are the result of the world data approximation by the function $\sim s^{-16}$.

The results are in a qualitative agreement with the behavior of the world data. The significant discrepancy between the data and CCR is at $\sqrt{s} < 3.1$ and $\sqrt{s} > 3.4$ GeV. However, this discrepancy is decreased with the scattering angle increasing.

5 Conclusion

The differential cross section data for dp-elastic scattering at 500, 750 and 900 MeV/n are obtained. The results are in a reasonable agreement with the world data obtained at the similar energies.

The obtained data were also compared with the calculations of the relativistic multiple scattering model. The best agreement is at 500 MeV/n. The discrepancies between the experimental data and theoretical predictions are increasing as the energy grows.

The differential cross section of dp-elastic scattering at the fixed scattering angle was obtained. The data cover the total c.m. energy range $\sqrt{s}$ = 3.1 - 3.42 GeV. The results are in a qualitative agreement with the behavior of the world data as well as with the prediction of CCR.

Acknowledgments. The work has been supported in part by the RFBR under grant $N^0$16-02-00203a, by the Ministry of Education, Science, Research, and Sport of the Slovak Republic (VEGA Grant No. 1/0113/18), by JINR- Slovak Republic and JINR-Romania scientific cooperation programs in 2016-2018.

References

[1] K. Ermisch et al., Phys. Rev. C **71**, 064004 (2005)
[2] K. Sekiguchi et al., Phys. Rev. C **65**, 034003 (2002)
[3] J.C. Alder et al., Phys. Rev. C **6**(6), 2010 (1972)
[4] N. E. Booth et al. Phys Rev D **4**, 1261 (1971)
[5] J.S. Vincent et al., Phys. Rev. Lett. **24**(5), 236 (1970)
[6] E. Culmez et al., Phys. Rev. C **43**(5), 2067 (1991)
[7] A.A. Terekhin et al., Eur. Phys. J. A **48**, 182 (2012)
[8] E. Winkelmann et al., Phys. Rev. C **21**, 2535 (1980)
[9] G.W. Bennet et al., Phys. Rev. Lett. **19**, 387 (1967)
[10] P.K. Kurilkin et al., PoS Baldin ISHEPP **XXI**, 040 (2012)
[11] A. Kievsky, M.Viviani, S.Rosati, Phys.Rev. C **64**, 024002 (2001)
[12] M. Viviani, A.Kievsky, S.Rosati, Few-Body Syst. **30**, 39 (2001)
[13] A. Deltuva et al., Phys.Rev. C **71**, 064003 (2005)
[14] H. Witala, Th.Cornelius, W.Glockle, Few-Body Systems **3**, 123 (1988)
[15] J.L. Friar et al. Phys.Rev. C **51**, 2356 (1995)
[16] W. Glockle et al., Phys.Rep. **274**, 107 (1996)
[17] J. Kuros-Zolnierczuk, H.Witala et al., Phys.Rev. C **66**, 024004 (2002)
[18] V. Franco, R.J.Glauber, Phys. Rev. Lett. **16**, 944 (1966)
[19] V. Franco, E.Coleman, Phys.Rev.Lett. **17**, 827 (1966)
[20] E.Bleszynski et al., AIP Conf. **150**, 1208 (1986)
[21] N.B. Ladygina et al., Eur. Phys. J. A **42**, 91 (2009)
[22] N. B. Ladygina Phys. Atom. Nucl. **71**, 2039 (2008)
[23] N.B. Ladygina Int. J. Mod. Phys. A **26**, 728 (2011)
[24] N. B. Ladygina, Eur.Phys.J. A **52**, 199 (2016)
[25] A.I. Malakhov et al., Phys. Res. A **440**, 320 (2000)
[26] A. A. Terekhin et al. Yad. Pfys. **6**, 1000 (2017)
[27] A. A. Terekhin et al. Phys. Part. Nucl. Lett. **12**, 695 (2015)
[28] http://afi.jinr.ru
[29] I. Froehlich et al Eur. Phys. J. A **45**, 401 (2010)
[30] V.A. Matveev et al. Lett. Nuovo Cimento **7**, 719 (1973)